J Appl Electrochem (2014) 44:841–848
DOI 10.1007/s10800-014-0692-0

RESEARCH ARTICLE

Effect of current density and sulfuric acid concentration on persulfuric acid generation by boron-doped diamond film anodes

Jake R. Davis · James C. Baygents · James Farrell

Received: 7 February 2014 / Accepted: 28 April 2014 / Published online: 14 May 2014

Abstract This research investigated the effects of current density and sulfuric acid concentration on the rates of persulfate generation by boron-doped diamond film anodes. Also investigated was the maximum conversion of sulfate to persulfate that could be achieved from electrolysis of sulfuric acid. Experiments were performed in batch systems using a rotating disk electrode (RDE) and a flow-through reactor with parallel plate electrodes. Both the RDE and flow-through experiments showed that there was a linear relationship between persulfate generation rates and current density. Persulfate generation rates became current limited at sulfuric acid concentrations of 2.25 M and above; however, Faradaic efficiencies under current-limited conditions were only $\sim$60 %, and were only weakly dependent on the current density. Persulfate generation rates in the flow-through reactor showed similar dependencies on current density and sulfuric acid concentration as those in the RDE reactor, but were 20–50 % lower. Acid catalyzed and thermal decomposition of persulfate limited the maximum conversion of sulfate to persulfate. A maximum fractional conversion of 78 % was achieved using an initial sulfuric acid concentration of 0.77 M. Surprisingly, this value was independent of the current density over the range of 100–300 mA cm^{-2}.

Keywords Sulfuric acid · Persulfate · Electrochemical · Electrosynthesis · Boron-doped diamond · BDD Anode

J. R. Davis · J. C. Baygents · J. Farrell (✉)
Department of Chemical & Environmental Engineering, University of Arizona, Tucson, AZ 85721-0011, USA
e-mail: farrellj@email.arizona.edu

1 Introduction

Peroxodisulfate ($S_2O_8^{2-}$), also known as persulfate, is the strongest oxidant of the peroxygen family of compounds, which includes the commonly used bleaching and disinfecting compounds peroxomonosulfate and peroxycarbonate [1]. The standard reduction potential (E^o) for persulfate to sulfate is 2.01 V, which is greater than that for hydrogen peroxide ($E^o = 1.8$ V) and permanganate ($E^o = 1.7$ V) [2]. Persulfate can act as an oxidant via thermal or radiation-induced decomposition into two sulfate radicals ($SO_4^{-\bullet}$). The sulfate radical is one of the strongest aqueous phase oxidants, with a standard reduction potential of 2.43 V, which is close to that for the hydroxyl radical ($E^o = 2.7$ V) [3].

At the industrial scale, persulfate is produced electrochemically via electrolysis of sulfate containing solutions using platinum electrodes at current densities greater than 500 mA cm^{-2} [4]. Several investigators have shown that persulfate can also be produced from oxidation of sulfuric acid using boron-doped diamond (BDD) film electrodes. In the earliest study, Michaud et al. [5] used an undivided flow-through cell to produce persulfate at a current density of 30 mA cm^{-2}. In order to investigate the mechanism for persulfate production, Serrano et al. [6] used a similar undivided flow-through cell to generate persulfate from sulfuric acid. All experiments were performed at a constant current density of 23 mA cm^{-2}. They proposed a mechanism involving the reaction of $HO^{\bullet}$ with HSO_4^- and H_2SO_4 to produce $SO_4^{-\bullet}$. Persulfate could then be produced via coupling of two $SO_4^{-\bullet}$ species. In both studies, the fraction of sulfate that was converted to persulfate was $<$5 %. The low conversion in these studies was desired in order to avoid persulfate reduction at the cathode and to limit decomposition of persulfate.

In alkaline, neutral, and dilute acid solutions, persulfate decomposes primarily via the overall reaction [6]:

$$S_2O_8^{2-} + H_2O \rightarrow 2 \cdot HSO_4^- + \frac{1}{2} \cdot O_2 \quad (1)$$

In more concentrated acid solutions, persulfate decomposition involves the reactions:

$$H_2S_2O_8 + H_2O \rightarrow H_2SO_5 + H_2SO_4 \quad (2)$$

$$H_2S_2O_8 + 2 \cdot H_2O \rightarrow H_2O_2 + 2 \cdot H_2SO_4 \quad (3)$$

The products of these reactions, peroxomonosulfuric acid (H_2SO_5) and hydrogen peroxide (H_2O_2) are also strong oxidants.

Due to its instability in aqueous solutions, persulfate is normally sold as a sodium, potassium, or ammonium salt; however, there are some applications where on-site generation of persulfate from sulfuric acid solutions may be desirable. In applications requiring the addition of both acid and oxidants, conversion of sulfuric acid to persulfuric acid using an electrochemical cell may provide a simple process for pH adjustment and disinfection. Evaporative cooling is one possible application, since acid is generally added to prevent scale formation, and disinfection and organic compound oxidation are also desired. The combination of acid with persulfate may also be useful in the mining industry for the heap leaching of chalcopyrite ores [8], and in swimming pools for pH adjustment, disinfection, and organic compound oxidation [9].

The overall goal of this study was to evaluate the technical and economic feasibility for point of use persulfate generation from sulfuric acid solutions using BDD anodes. To that end, the effect of current density and sulfuric acid concentration on the rates and Faradaic efficiencies for persulfate production was investigated using batch and flow-through reactors. As part of the feasibility evaluation, the maximum conversion of sulfate to persulfate that could be achieved from electrolysis of sulfuric acid solutions was investigated. An economic evaluation of the energy requirements associated with the process was also performed.

2 Experimental

2.1 Reagents and analysis

All experiments employed reagent grade sulfuric acid, peroxodisulfate, and peroxomonosulfate obtained from Fisher Scientific, and 18 MΩ cm ultrapure water. Sulfuric acid concentrations were determined using a gravimetric method based on the solution density at 25 °C. Peroxodisulfate, peroxomonosulfate, and sulfate ion concentrations were determined using a Dionex ICS-5000 ion chromatograph equipped with a Dionex AS-16-2 column. An eluent gradient program with a 0.375 cm^3 min^{-1} isocratic flow permitted simultaneous analysis of sulfate, peroxodisulfate, and peroxomonosulfate. The generation of ozone by the BDD anodes was investigated by comparing persulfate concentrations in samples that were vigorously purged with nitrogen gas immediately after sampling to concentrations in identical samples that were not purged. A decline in the persulfate concentration in the unpurged samples versus the purged samples would be indicative of reaction with anodically produced ozone.

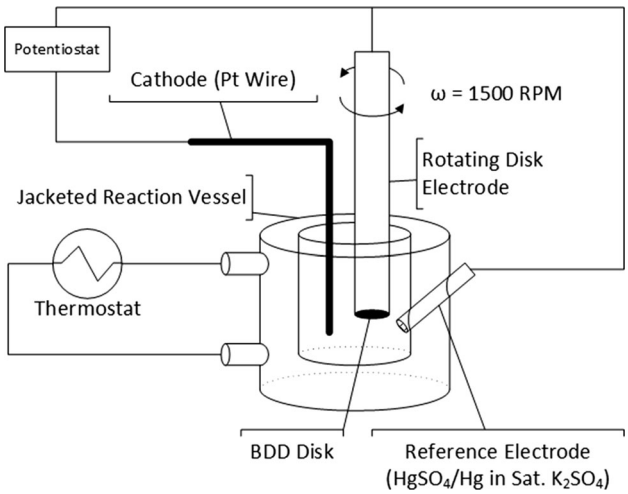

Fig. 1 Diagram of RDE experiment apparatus

Solutions were sampled using a 5 mL pipette and 5 mL Dionex autosampler vials and analyzed in triplicate. Samples were immediately analyzed to minimize persulfate decomposition. However, at acid concentrations >3 M, the measured concentration of persulfate had to be corrected for acid-catalyzed decomposition. This correction was performed by measuring the pseudo-first-order rate constant for persulfate degradation [7] in separate experiments. After correcting for decomposition, the typical relative standard deviation of intra-sample injections was ~3 %. Concentrations reported here are the mean of the triplicate analyses.

2.2 Rotating disk electrode experiments

The working electrode consisted of a BDD film on a p-silicon substrate with a surface area of 1 cm^2, and was provided by Advanced Diamond Technologies. The electrode was housed in a Princeton Applied Research (PAR) model 616 rotating disk electrode (RDE) assembly. To eliminate mass transfer limitations, the RDE was rotated at 1500 rpm. Currents or potentials were controlled using a Gamry Series G model 750 potentiostat/galvanostat. A 5-cm long by 0.3-mm diameter platinum wire served as the counter electrode. A PAR mercury/mercury sulfate

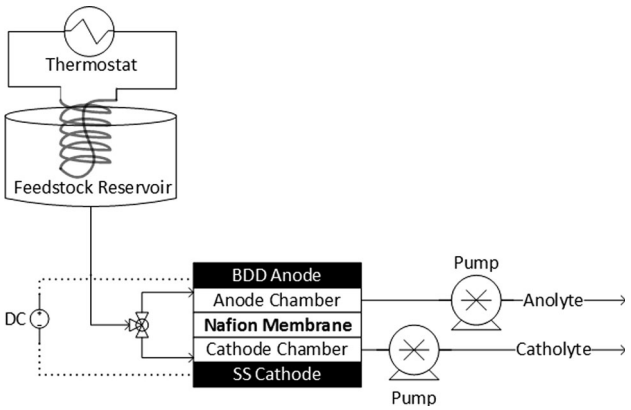

Fig. 2 Diagram of differential experiment apparatus

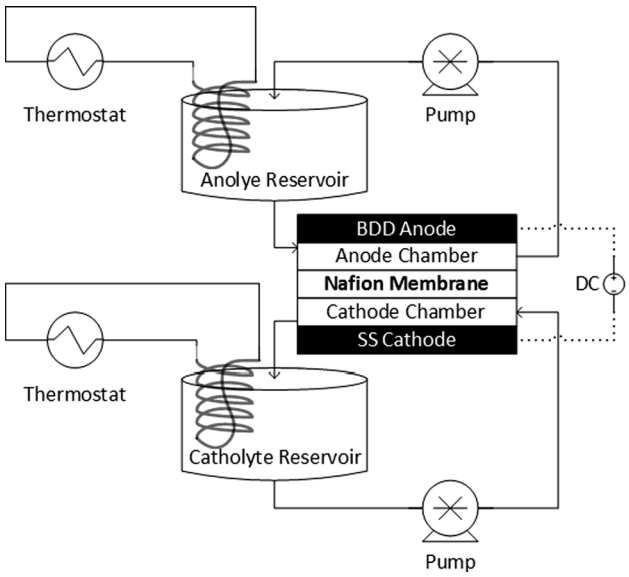

Fig. 3 Diagram of recirculation experiment apparatus

electrode (MSE) saturated with potassium sulfate (E^o = 0.654 V) served as the reference. The RDE experiments were performed in a jacketed Pyrex® reactor containing 50 mL of sulfuric acid maintained at 20 °C using a recirculating water bath. The electrolysis time was 5 min and current densities ranged from 10 to 280 mA cm^{-2}. Individual experiments were conducted for each combination of sulfuric acid concentration and current density (Fig. 1).

2.3 Differential reactor experiments

Experiments were also performed using a MicroFlow Cell® parallel plate, flow-through reactor obtained from Electrocell®. The anode consisted of a BDD film on a 3-mm-thick niobium metal substrate, and was obtained from Advanced Diamond Technologies. A 3-mm-thick stainless steel plate served as the cathode, and a Nafion® membrane was used to separate the anode and cathode chambers. Viton® gaskets with a thickness of 1 mm were used as cell spacers, and the exposed area for each electrode was 9 cm^2.

Electrolysis experiments were performed galvanostatically at current densities ranging from 10 to 300 mA cm^{-2}. Polarizations ranging from 4 to 6.5 V were applied using a GW Instek SPS-606 power supply. A single thermostated reservoir served to provide the anolyte and catholyte feed solutions. All experiments were performed using peristaltic pumps with Viton® tubing at anolyte and catholyte flow rates of 100 mL min^{-1}, yielding a mean hydraulic detention time of 0.5 s. Effluent samples from the reactor were taken at two-minute intervals using an autosampler (Fig. 2).

2.4 Recirculation reactor experiments

Experiments were performed to determine the maximum conversion of sulfate to persulfate using the flow-through reactor described above. Separate thermostated reservoirs were used for the anolyte and catholyte. Peristaltic pumps operating at 100 mL min^{-1} were used to circulate the anolyte and catholyte solutions between the reactor chambers and the electrolyte reservoirs. The reactor was operated galvanostatically for periods ranging from 1 week to 1 month. Samples of the anolyte and catholyte were taken periodically using a 5 mL pipette. Fluid levels in the anolyte and catholyte reservoirs were monitored daily to correct measured solution concentrations for osmotic and electro-osmotic flows between the cell chambers (Fig. 3).

3 Results and discussion

3.1 Rotating disk electrode

Figure 4 shows the rate of persulfate generation as a function of current density for sulfuric acid concentrations ranging from 0.30 to 2.5 M in the RDE reactor. The rates of persulfate generation were linearly proportional to the current density for all concentrations tested. Table 1 shows the linear regression coefficients and the coefficients of determination for the datasets in Fig. 4. The linear regression coefficients indicate that the rate of persulfate generation increased with H_2SO_4 concentrations in a manner that is consistent with the reaction becoming increasingly current limited with increasing H_2SO_4 concentration.

Figure 5 shows this same data as Fig. 4 plotted as the natural logarithm of the persulfate production rate versus the electrode potential. If the persulfate production rate followed Butler–Volmer kinetics [10], the dataset for each concentration would be expected to fall on a straight line,

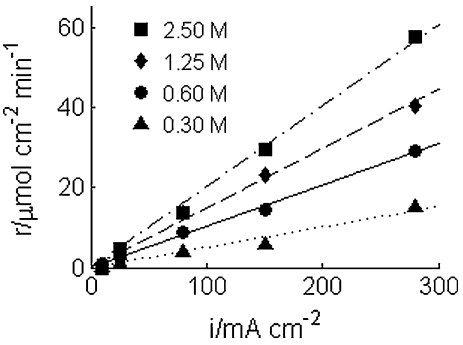

Fig. 4 Persulfate production rate (r) as a function of current density (i) for sulfuric acid concentrations of 2.50 M (*square*), 1.25 M (*diamond*), 0.60 M (*circle*), 0.30 M (*triangle*) at $T = 20$ °C. *Lines* represent linear regressions

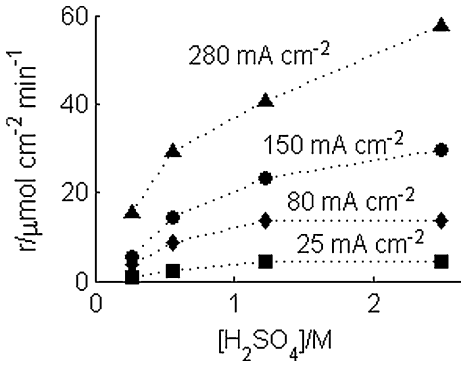

Fig. 6 Persulfate production rate (r) as a function of bulk sulfuric acid concentration at current densities of 25 mA cm^{-2} (*square*), 80 mA cm^{-2} (*diamond*), 150 mA cm^{-2} (*circle*), 280 mA cm^{-2} (*triangle*) at $T = 20$ °C

Table 1 Linear regression coefficients [β_1 (μmol mA^{-1} min^{-1})] and coefficients of determination (R^2) for the persulfate production rate data shown in Fig. 4 for various sulfuric acid concentrations [H_2SO_4 (M)]

H_2SO_4 (M)	β_1 (μmol mA^{-1} min^{-1})	R^2
0.30	0.051	0.964
0.60	0.103	0.997
1.25	0.148	0.994
2.50	0.202	0.994

All regressions models have been forced through the origin

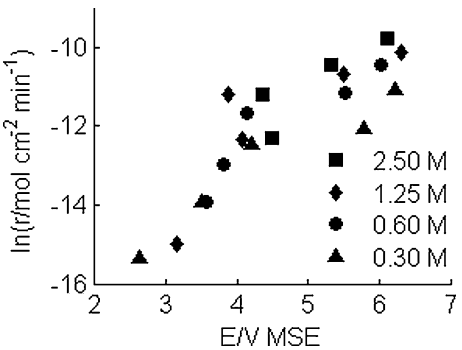

Fig. 5 Natural logarithm of the persulfate production rate (r) as a function of electrode potential (E) for sulfuric acid concentrations of 0.30 M (*triangle*), 0.60 M (*circle*), 1.25 M (*diamond*), 2.50 M (*square*) at $T = 20$ °C

and the datasets for all concentrations would be expected to have the same slope. The lack of conformance to the Butler–Volmer equation suggests that a complex series of reactions control the rate of persulfate production.

Figure 6 shows the persulfate production rate as a function of the concentration of H_2SO_4 added to the solution. At current densities of 25 and 80 mA cm^{-2}, the persulfate production rate reached a maximum value at an H_2SO_4 concentration of 1.25 M. This plateau in the production rate is indicative of a current-limited reaction. A plateau in the persulfate production rate at H_2SO_4 concentrations between 1 and 2 M was also observed by Serrano et al. [6] at a current density of 23 mA cm^{-2}. At current densities of 150 and 280 mA cm^{-2}, the plateau in the production rates was not attained for the concentrations tested.

The Faradaic efficiency, defined as the fraction of the current producing persulfate, can be determined using a two-electron oxidation for converting sulfate to persulfate. Figure 7 shows the Faradaic efficiencies for the data in Figs. 4, 5, and 6. Since there were no other sulfate oxidation products or ozone generation observed, the Faradaic losses can be attributed to oxygen evolution. The efficiencies appear to be only weakly correlated with the current density, as illustrated by the low coefficients of determination (R^2) for the linear fits shown in Table 2. As expected, the Faradaic efficiencies increase with increasing H_2SO_4 concentration. The efficiency for the 2.5 M H_2SO_4 concentration of $\sim$60 % is considerably lower than the 95 % efficiency observed by Serrano et al. [6] at the same concentration. The lower efficiency observed in Fig. 7 may be a result of the 20 °C temperature used here, as compared to 9 °C used by Serrano et al. [6], who reported that their current efficiencies decreased with increasing temperature. Additionally, as previous investigations have shown, differences in BDD surface chemistry may also contribute to differences in Faradaic efficiency [11, 12].

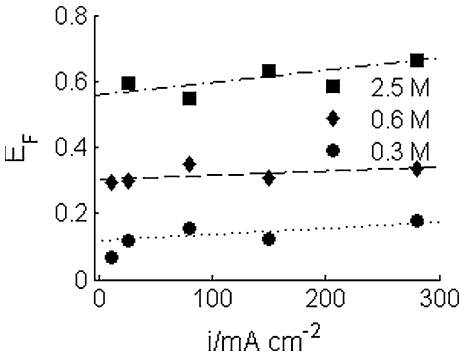

Fig. 7 Faradaic efficiency (E_F) as a function of current density (i) in 0.30 M (*circle*), 0.60 M (*diamond*), and 2.50 M (*square*) sulfuric acid at $T = 20$ °C. *Lines* represent linear regressions

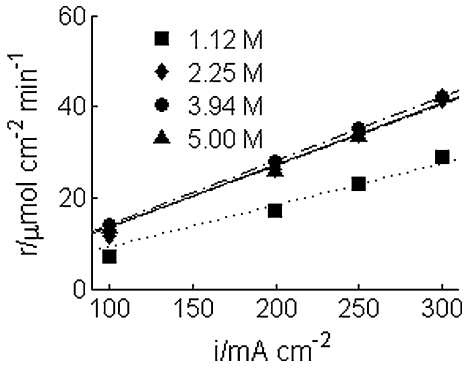

Fig. 9 Persulfate production rate (r) as a function of current density (i) in a differential flow-through cell with bulk sulfuric acid concentrations of 1.12 M (*square*), 2.25 M (*diamond*), 3.94 M (*circle*), 5 M (*triangle*) at 15 °C. *Lines* represent linear regressions

Table 2 Linear regression coefficients [β_1 (mA^{-1} cm^2)], intercept values (β_2), and coefficients of determination (R^2) for the Faradaic efficiency (E_F) data shown in Fig. 7 for various sulfuric acid concentrations [H_2SO_4 (M)]

H_2SO_4 (M)	β_1 (mA^{-1} cm^2)	β_2	R^2
0.30	0.0002	0.1182	0.4987
0.60	0.0001	0.3029	0.3346
2.50	0.0004	0.5590	0.6486

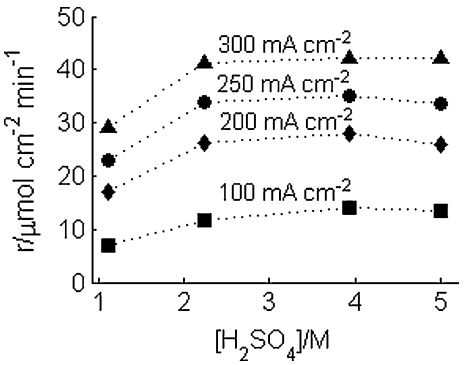

Fig. 8 Persulfate production rate (r) as a function of bulk sulfuric acid concentration in a differential flow-through cell at current densities of 100 mA cm^{-2} (*square*), 200 mA cm^{-2} (*diamond*), 250 mA cm^{-2} (*circle*), 300 mA cm^{-2} (*triangle*) at *15* °C

3.2 Differential flow-through reactor

Single-pass experiments were performed to determine the effect of fluid mechanics on rates and Faradaic efficiencies for persulfate production. These experiments were performed at a sufficiently high flow rate such that less than 0.1 % of the sulfate was converted to persulfate during a single pass through the cell. Under these conditions, the electrochemical cell can be considered as a differential reactor, and the H_2SO_4 concentration can be considered constant. Figure 8 shows the persulfate production rates as a function of the bulk H_2SO_4 concentration for current densities ranging from 100 to 300 mA cm^{-2}. The persulfate production rates in the flow-through reactor reached their maximum current-limited values at a H_2SO_4 concentration of 2.25 M. At equivalent current densities and H_2SO_4 concentrations, the persulfate production rates in the flow-through reactor were from 20 to 50 % lower than those observed in the RDE.

Table 3 Linear regression coefficients [β_1 (μmol mA^{-1} min^{-1})] and coefficients of determination (R^2) for the persulfate production rate data show in Fig. 9 for various sulfuric acid concentrations [H_2SO_4 (M)]

H_2SO_4 (M)	β_1 (μmol mA^{-1} min^{-1})	R^2
1.12	0.092	0.968
2.25	0.135	0.991
3.94	0.140	1.00
5.00	0.136	0.992

Figure 9 shows the persulfate production rates as a function of the current density for H_2SO_4 concentrations ranging from 1.12 to 5 M. At all concentrations, the production rates were a linear function of the current density, as illustrated by the high R^2 values for the linear regressions shown in Table 3. This is the same behavior as that observed with the RDE. At all current densities, the persulfate production rates were nearly identical for H_2SO_4 concentrations of 2.25 M and above. The absence of any effect of H_2SO_4 concentration indicates that diffusional mass transfer effects were not limiting the persulfate production rates at H_2SO_4 concentrations greater than 2.25 M. One factor that may contribute to lower persulfate production rates in the flow-through versus the RDE reactor is

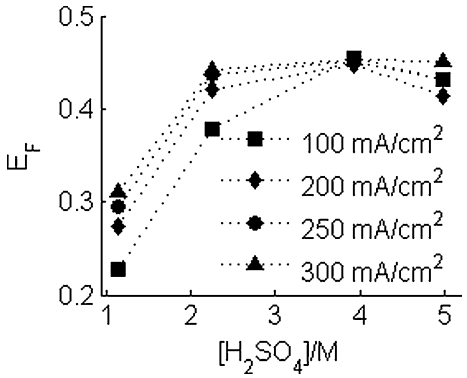

Fig. 10 Faradaic efficiency (E_F) as a function of bulk sulfuric acid concentration in a differential flow-through cell, at current densities of 100 mA cm^{-2} (*square*), 200 mA cm^{-2} (*diamond*), 250 mA cm^{-2} (*circle*), 300 mA cm^{-2} (*triangle*) at 15 °C

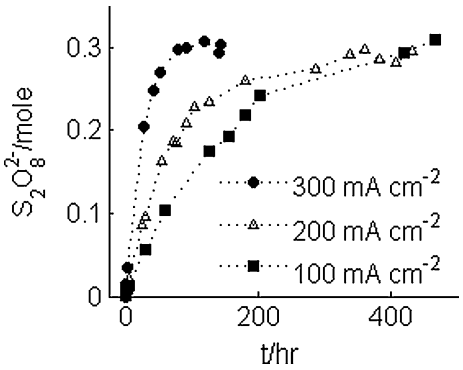

Fig. 11 Amount of persulfate produced as a function of time (t) in a recirculating system at current densities of 100 mA cm^{-2} (*square*), 200 mA cm^{-2} (*triangle*), 300 mA cm^{-2} (*circle*) at 20 °C and an initial sulfuric acid concentration of 0.77 M

differences in the electrode properties. Chaplin et al. [11, 12] have shown that BDD anode surface chemistry, morphology, and electrochemical character are highly dependent on electrode age, history, and fabrication. While fabrication was done in an identical fashion, no other measures were taken to assure similitude between the disk and plate electrodes. This has likely lead to their apparent electrochemical dissimilarities.

Figure 10 shows the Faradaic efficiency for persulfate production for the data in Figs. 8 and 9. The Faradaic efficiencies in the flow-through reactor displayed similar trends as those observed with the RDE, but were consistently ~25 % lower than the RDE efficiencies. The decline in efficiency associated with increasing the H_2SO_4 concentration from 4 to 5 M may be an artifact of the acid-catalyzed persulfate destruction.

3.3 Recirculation flow-through reactor

Acid-catalyzed persulfate degradation will be important in systems trying to produce useful concentrations of persulfate. The rate of acid-catalyzed decomposition was found to be first order in the persulfate concentration and was a strong function of the acid concentration. Experiments using separate recirculating anolyte and catholyte solutions were performed to determine the practicality of producing persulfate from sulfuric acid. Figure 11 shows the moles of persulfate in the anolyte solutions as a function of electrolysis time for the recirculating experiments with initial H_2SO_4 concentrations of 0.77 M at current densities of 100, 200, and 300 mA cm^{-2}. Due to electro-osmotic and osmotic flow between chambers, the volume of the anolyte solutions declined over time from 1 L to approximately 0.5 L. Persulfate concentrations were also monitored in the catholyte solution and were found to be near the method

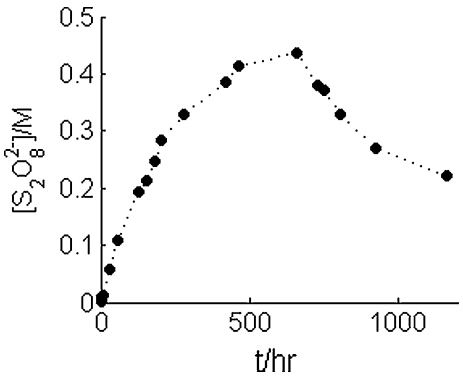

Fig. 12 Persulfate production at 100 mA cm^{-2} and decay beginning at 661 h in a recirculating system at 20 °C . Initial H_2SO_4 concentration of 0.77 M

detection limit of 10 mg L^{-1}. Peroxomonosulfate concentrations were also found to be below the method detection limit of 5 mg L^{-1}. At all three current densities, the maximum amount of persulfate that could be obtained from one liter of 0.77 M H_2SO_4 was ~0.30 mol. This represents conversion of 78 % of the initially present sulfate species into persulfate. The initial persulfate production rates in Fig. 11 were similar to those observed in the single-pass flow-through experiments. However, with increasing elapsed time, the observed rate of persulfate production appeared to decline. This apparent decline in production rate can be attributed to both decreasing sulfate concentrations and to increasing rates of persulfate decomposition.

The effect of persulfate decomposition on measured persulfate concentrations can be seen in Fig. 12, which shows the persulfate concentrations as a function of elapsed time for an anolyte solution with an initial H_2SO_4 concentration of 0.77 M. In this experiment, a current density of 100 mA cm^{-2} was used for the initial 661 h and

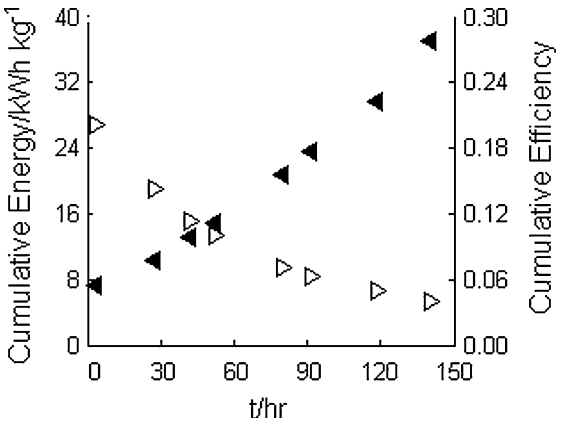

Fig. 13 Cumulative specific energy (*solid triangle*) of persulfate and cumulative efficiency (*open triangle*) as a function of time in a recirculating system with an initial sulfuric acid concentration of 0.77 M and current density of 300 mA cm^{-2} at 20 °C

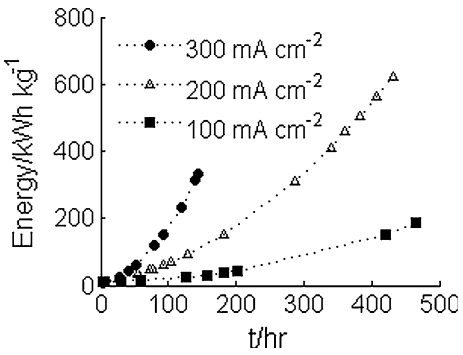

Fig. 14 Instantaneous specific energy for persulfate as a function of time in a recirculating system with an initial sulfuric acid concentration of 0.77 M at 20 °C

after that time, the current was turned off. Upon termination of the current, the persulfate concentrations declined at a rate that can be approximated by a first-order process with a pseudo-first-order rate constant of 2.5×10^{-5} min^{-1}. This decay rate is equivalent to that predicted by Johnson et al. [13] for pH of 0.68 at 20 °C.

3.4 Energy requirements

The economic feasibility for on-site persulfate generation will depend on the energy costs. The energy required per kg of persulfate generated can be determined from the data in Fig. 11. Figure 13 shows the cumulative Faradaic current efficiencies and the cumulative energy requirement per kg of persulfate generated using a current density of 300 mA cm^{-2} and initial sulfuric acid concentration of 0.77 M. The initial Faradaic efficiency of 20 % declined to 10 % by 52 h elapsed. This can be attributed to conversion of 70 % of the sulfate species (SO_4^{2-}, HSO_4^-, H_2SO_4) into persulfate, and the increasing rate of persulfate decay.

Figure 14 shows the instantaneous energy requirement per kg of persulfate generated using a current densities of 100, 200, and 300 mA cm^{-2}. When purchased in 25 kg containers, the cost including freight, from Santa Ana, California to Tucson, Arizona, for sodium persulfate is ~$6.70 kg^{-1}. Figure 14 suggests that on-site production of persulfate by oxidizing sulfuric acid with BDD electrodes can provide a cost advantage over purchasing bulk sodium persulfate. For example, at a current density of 300 mA cm^{-2} and an electrolysis time of 50 h, the energy requirement for producing persulfuric acid from sulfuric acid is 14.8 kWh/kg. For an energy cost of $0.10 per kWh, this cost of $1.48 is 22 % of the commodity chemical cost for persulfate. At this point, 70 % of the total sulfate species (SO_4^{2-}, HSO_4^-, H_2SO_4) have been converted to persulfate.

4 Conclusions

This research showed that rates of persulfate production depended linearly on the applied current in both RDE and flow-through reactors. The Faradaic efficiencies depended on the sulfuric acid concentration, and in the flow-through reactor never exceeded 0.45, even when under current-limited conditions at high H_2SO_4 concentrations. The maximum fractional conversion of sulfate ions to persulfate is limited by acid-catalyzed persulfate decomposition, and high conversions can only be achieved at low acid concentrations. Since electrolyzing sulfuric acid to produce persulfate does not significantly impact the solutions acidity, applications requiring the addition of both acid and oxidants may benefit from on-site persulfate production.

Acknowledgments Funding for this work was provided by the National Science Foundation Small Business Innovative Research Program through Award 1058505.

References

1. Jakob H, Leininger S, Lehmann T, Jacobi S, Gutewort S (2007) Peroxo compounds, inorganic. Ullmann's encyclopedia of industrial chemistry. Wiley-VCH, Weinheim
2. Lide D (1990) CRC handbook of chemistry and physics, 71st edn. CRC Press, Boca Raton
3. Steiner N, Eul W (2006) Peroxides, inorganic. Kirk-Othmer encyclopedia of chemical technology, 5th edn. Wiley, New York
4. Radimer K, McCarthy M (1979) US Patent 4,144,144
5. Michaud P, Mahe' E, Haenni W, Perret A, Comninellis C (2000) Preparation of peroxodisulfuric acid using boron-doped diamond thin film electrodes. Electrochem Solid State Lett 3:77–79
6. Serrano K, Michaud P, Comninellis C, Savall A (2002) Electrochemical preparation of peroxoidsulfuric acid using boron

doped diamond thin film electrodes. Electrochim Acta 48:431–436
7. Kolthoff I, Miller I (1951) The chemistry of persuflate: I. The kinetics and mechanism of the decomposition of the persulfate ion in aqueous medium. J Am Chem Soc 73:3055–3059
8. Dakubo F, Baygents J, Farrell J (2012) Peroxodisulfate assisted leaching of chalcopyrite. Hydrometallurgy 121–124:68–73
9. Wojtowicz J (2001) Survey of swimming pool/Spa sanitizers and sanitation systems. J Swim Pool Spa Ind 4(1):9–29
10. Hamann C, Hamnett A, Vielstich W (2007) Electrochemistry. Wiley, Weinheim
11. Chaplin B, Hubler D, Farrell J (2013) Understanding anodic wear at boron doped diamond film electrodes. Electrochim Acta 89:122–131
12. Chaplin B, Wyle I, Zeng H, Carlisle J, Farrell J (2011) Characterization of the performance and failure mechanisms of boron-doped ultrananocrystalline diamond electrodes. J Appl Electrochem 41(11):1329–1340
13. Johnson R, Tratnyek P, Johnson R (2008) Persulfate persistence under thermal activation conditions. Environ Sci Technol 42:9350–9356